

# Programmable autonomous synthesis of single-stranded DNA

Jocelyn Y. Kishi<sup>1,2</sup>, Thomas E. Schaus<sup>1,2</sup>, Nikhil Gopalkrishnan<sup>1,2</sup>, Feng Xuan<sup>1,2</sup> and Peng Yin<sup>1,2\*</sup>

**DNA performs diverse functional roles in biology, nanotechnology and biotechnology, but current methods for autonomously synthesizing arbitrary single-stranded DNA are limited. Here, we introduce the concept of primer exchange reaction (PER) cascades, which grow nascent single-stranded DNA with user-specified sequences following prescribed reaction pathways. PER synthesis happens in a programmable, autonomous, *in situ* and environmentally responsive fashion, providing a platform for engineering molecular circuits and devices with a wide range of sensing, monitoring, recording, signal-processing and actuation capabilities. We experimentally demonstrate a nanodevice that transduces the detection of a trigger RNA into the production of a DNAzyme that degrades an independent RNA substrate, a signal amplifier that conditionally synthesizes long fluorescent strands only in the presence of a particular RNA signal, molecular computing circuits that evaluate logic (AND, OR, NOT) combinations of RNA inputs, and a temporal molecular event recorder that records in the PER transcript the order in which distinct RNA inputs are sequentially detected.**

DNA is the information carrier for life and encodes the instructions for diverse molecular functions in the genome. DNA is also a foundational element in nanotechnology, and is used to construct nanostructures<sup>1–11</sup> and dynamic circuits and devices<sup>12–20</sup> with diverse technological applications<sup>21–32</sup> (for example, to spatially organize inorganic and organic materials for nanofabrication and biomedical applications<sup>23,24,27</sup>, for super-resolution imaging<sup>26</sup> and as single-molecule tools<sup>25,31,32</sup>). DNA is also widely used in biotechnology applications<sup>33–38</sup>, such as biosensing, sequence amplification, genome editing and even memory storage.

Despite the diverse applications of DNA in biology, nanotechnology and biotechnology, current programmable methods for autonomously synthesizing single-stranded sequences are limited. DNA oligos are typically synthesized non-autonomously through a staged process that uses specific chemical conditions at each of several externally controlled steps<sup>39</sup>. Enzyme-driven methods like the polymerase chain reaction (PCR)<sup>40</sup>, loop-mediated isothermal amplification (LAMP)<sup>35</sup>, strand displacement amplification (SDA)<sup>33</sup>, rolling circle amplification (RCA)<sup>34</sup> and polymerase/exonuclease/nickase (PEN) reactions<sup>41,42</sup> are typically limited to producing identical copies of fixed sequences. To overcome this limitation, we introduce primer exchange reaction (PER) cascades, which isothermally produce single-stranded DNA with arbitrary user-prescribed sequences in a programmable, autonomous, stepwise fashion with the aid of a strand-displacing polymerase. The PER cascade starts with a prescribed DNA primer. Using a catalytic DNA hairpin mediator, PER then appends to the existing primer a new primer with an independent, user-specified sequence (that is, a ‘primer exchange reaction’). The newly extended primer can then trigger the next step extension, thus forming a programmable PER cascade to autonomously grow a nascent DNA strand along a prescribed pathway to produce an arbitrary user-prescribed sequence (Fig. 1A). Although PEN reaction networks<sup>41,42</sup> also use a strand displacing polymerase (together with a nicking enzyme) to cascade one primer sequence into another, the PER cascades introduce the critical new capability of concatenating newly synthesized transcripts to grow a nascent DNA strand, which can serve diverse functional roles.

When, and only when, the right set of PER hairpins and the corresponding PER primer coexist is a new strand produced autonomously *in situ*. As the strand can be programmed to be of arbitrary user-specified sequence, it could serve many of the functional roles of DNA described above (for example, structural elements for nanoconstructs, templates for organizing materials, chemically active species and so on), providing a way for programmable *in situ* control/delivery of such functions. Additionally, by interfacing the PER hairpins with external molecular elements, each of these functional responses could be programmed to respond to different environmental cues (for example, the presence or absence of certain combinations of biomolecules, such as microRNAs; Fig. 1B–E). Such responsive synthesis could be used to implement molecular behaviours that are tailored to particular environmental contexts, enabling programmable dynamic molecular circuits with a wide range of molecular sensing, monitoring, recording, signal-processing and actuation capabilities.

Here, to explore these conceptual possibilities, we experimentally demonstrate several distinct types of molecular behaviour that can be implemented with PER cascades. These include a nanodevice that transduces the detection of a trigger RNA into the production of a DNAzyme that degrades an independent RNA substrate, a signal amplifier that conditionally synthesizes long fluorescent strands only in the presence of a particular RNA signal, molecular computing circuits that evaluate logic (AND, OR, NOT) combinations of RNA inputs, and a temporal molecular event recorder that records in the PER transcript the order in which distinct RNA inputs are sequentially detected. Collectively, these results suggest that the PER cascades could provide the basis for a new generation of programmable molecular devices.

## Results

**PER mechanism.** A PER reaction is patterned by a single catalytic PER hairpin (Fig. 2A), which prescribes the sequence (domain **b**) that becomes appended to primer strands with sequence domain **a**. Figure 2C depicts the PER reaction cycle. In step 1, a primer with sequence domain **a** binds to its complement **a\*** on the 3' end

<sup>1</sup>Wyss Institute for Biologically Inspired Engineering, Harvard University, Boston, Massachusetts 02115, USA. <sup>2</sup>Department of Systems Biology, Harvard Medical School, Boston, Massachusetts 02115, USA. \*e-mail: [py@hms.harvard.edu](mailto:py@hms.harvard.edu)

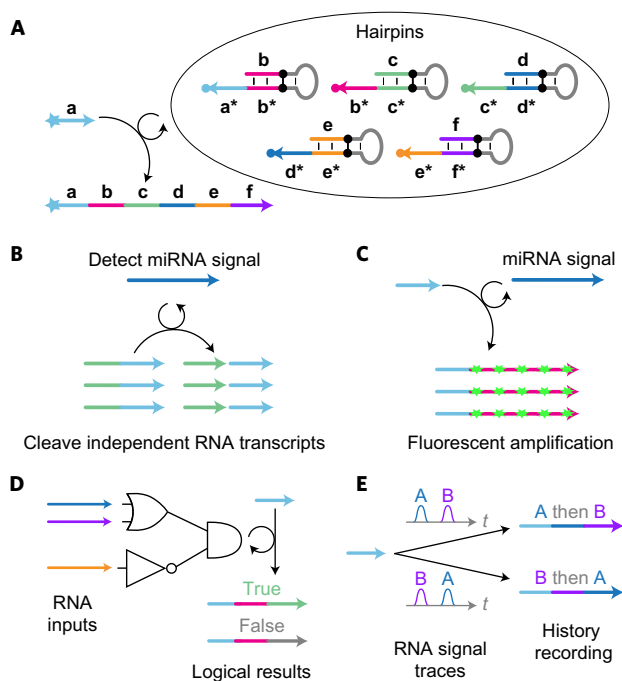


**Figure 1 | PER overview.** **A**, PER cascades grow nascent strands of single-stranded DNA (ssDNA) with prescribed sequences. **B**, A nanodevice synthesizes a functional DNAzyme that cleaves an independent transcript in response to an input miRNA signal. **C**, A PER signal amplifier conditionally synthesizes fluorescent strands only in the presence of a particular RNA signal. **D**, PER logic computation, which evaluates a logic expression based on which RNA inputs are present. **E**, A PER molecular program that records the order in which two signals are encountered in a DNA transcript.

of the primer. A strand-displacing polymerase can subsequently extend the primer by copying the **b** domain (which is termed the *copy* region of the PER hairpin) before halting at the stop sequence (step 2). The copied **b** domain is then able to compete with the **b** domain on the hairpin through the random walk process of three-way branch migration<sup>43</sup> (step 3). Finally, the extended primer can spontaneously dissociate from the hairpin

once the copied domain **b** has been displaced (step 4). The hairpin is then free to interact with another primer in another cycle of primer exchange. In our experiments, we use 7–9 nt (nucleotide) primer binding domains, which enable effective priming in steps 1–2 and permit efficient spontaneous dissociation in step 4 at 37 °C. The kinetics of this reaction are further characterized in Supplementary Section 1. Using a series of 2 min PER reactions with different hairpin concentrations, we found that the reaction can be roughly approximated as a bimolecular reaction between primers and hairpins with a rate constant of  $5.4 \times 10^5 \text{ M}^{-1} \text{ s}^{-1}$ .

Primer exchange hairpins were repurposed from the ‘copy-and-release hairpin’ that we recently described for the autocyclic proximity recording mechanism<sup>44</sup>. Each PER hairpin uses a stop sequence to halt polymerization<sup>45–48</sup>. For example, this stop sequence can be a G–C pair (Fig. 2B) if the **a** (blue) and **b** (pink) domains comprise a three-letter code of As, Ts and Cs, and dGTP is excluded from the mix. Other stop sequences include chemical modifications and synthetic base pairs, which permit all four letters to be synthesized (Fig. 4B and Supplementary Section 2). Primers can be labelled with a dye on their 5' ends for tracking in gel electrophoresis experiments (Fig. 2D). Hairpins also typically contain an inverted dT or other modification on their 3' ends to prevent their extension on the 5' unbound region of the primer (if any; not depicted), which could cause the primers to become irreversibly bound (data not shown).

Primers and hairpins were incubated together with Bst large fragment polymerase to validate and characterize the basic single PER (Fig. 2D). The system comprises two components, the fluorophore-labelled primer and hairpin depicted in Fig. 2B, and denaturing gel electrophoresis was used to track the progression of the basic PER. Lane 1 shows the band corresponding to the primer with no hairpin and lanes 2–11 depict the time progression of the PER at 10 min intervals with a 100:1 primer-to-hairpin ratio. These data confirm the catalytic recycling of the hairpin in solution. Bst large fragment polymerase, which has strong strand-displacing and no exonuclease activity, was the first polymerase we tried. As it worked well initially, we used it for all other systems for consistency. However, other non-exonuclease polymerases (for example, Klenow (exo-) and Bsm) were also observed to be compatible with PER (data not shown).

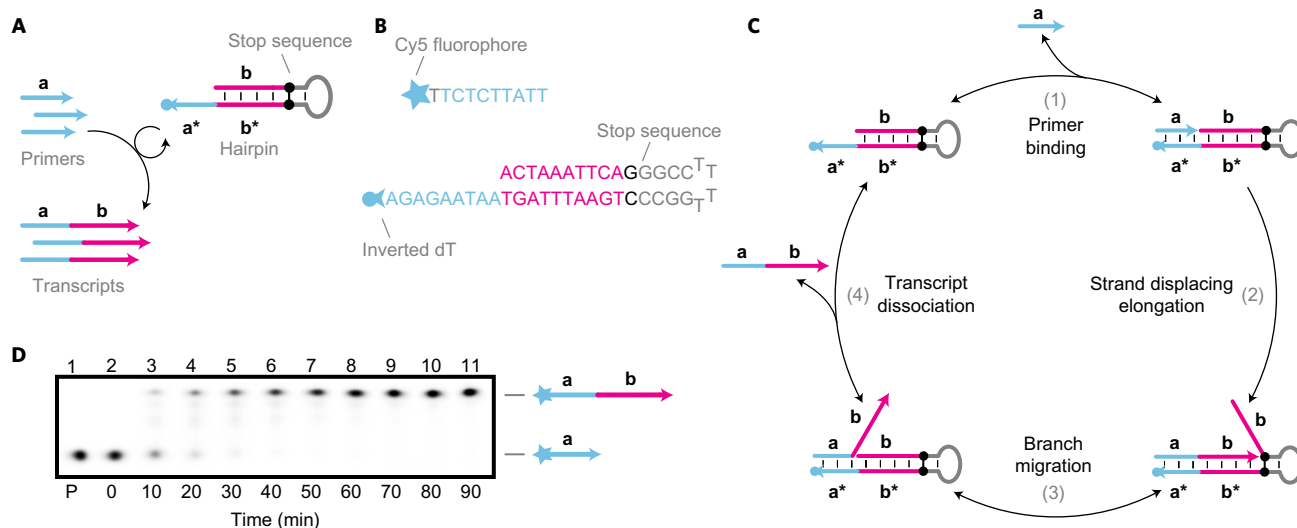


**Figure 2 | PER mechanism.** **A**, A PER, which uses a catalytic hairpin to produce transcripts of the form (A–B). **B**, An example reaction implementation with a hairpin that uses a G–C pair as a stop sequence. See Supplementary Section 2 for other types of stop sequences that can be used. **C**, The PER cycle. **D**, PAGE denaturing gel depicting a reaction time series of a primer exchange reaction. Primer and hairpin concentrations were fixed at 100 nM and 1 nM, respectively, and reactions were incubated at 37 °C with 10  $\mu\text{M}$  of dATP, dTTP and dCTP. See Methods and Supplementary Section 3 for additional details.

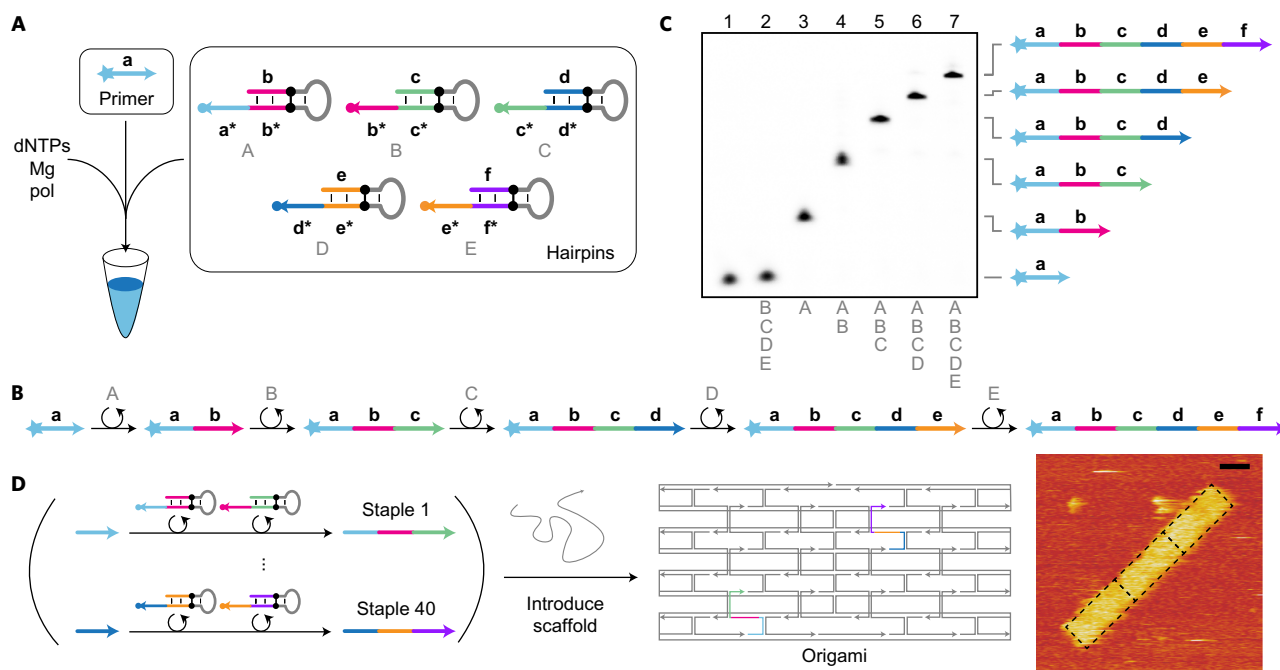


**Figure 3 | PER cascades.** **A**, Schematic for autonomous stepwise growth of a primer sequence. **B**, Reaction diagram for five elongation steps, patterned by hairpins A, B, C, D and E. **C**, Denaturing gel demonstrating differential extension with different subsets of the hairpin species present. Reactions were incubated for 4 h at 37 °C, with primers at 100 nM, hairpins at 10 nM and dATP, dTTP and dCTP at 10 μM each. **D**, Schematic for parallel synthesis of 40 staple strands for a DNA origami structure and AFM image of three of these structures aggregated with overlay of expected origami borders. Scale bar, 23 nm. PER synthesis reactions were incubated for 1 h at 37 °C, with primers at 100 nM, hairpins at 10 nM and dATP, dTTP and dCTP at 100 μM each. After heat inactivation, the scaffold was introduced directly to the reactions and structures were annealed from 80 to 20 °C over 1 h. See Methods and Supplementary Section 4 for additional details.

**PER cascades for synthesizing user-prescribed sequences.** PERs can be chained together to form PER cascades that grow DNA strands of fixed length and prescribed sequence following a prescribed reaction pathway. The first PER pathway we implemented was a cascade of five elongation steps mediated by a set of catalytic hairpin species (Fig. 3A). With all five hairpins and the primer present in solution, the pathway proceeds through five elongation steps (Fig. 3B). Hairpin A catalyses extension of the primer domain **a** with domain **b**. Hairpin B then catalyses the extension of domain **b** with domain **c**, and hairpins C–E catalyse the extension of **c** with **d**, **d** with **e**, and **e** with **f**, respectively.

Denaturing gel electrophoresis validated the ordered elongation of the primer strand when mixed with different subsets of the hairpins (Fig. 3C). Lane 1 shows a reaction where just the primer and no hairpins were incubated together. Lane 2 shows the primer incubated with hairpins B–E, which is all hairpins except the one that initiates the growth, hairpin A. This control shows no detectable leakage. Lane 3 shows the first elongation step with the primer and hairpin A incubated together. Lane 4 shows two elongations when the primer is incubated with the first two hairpins, A and B. Lanes 5, 6 and 7 show three, four and five elongation steps of the primer when incubated with hairpins A–C, A–D and A–E, respectively. The expected lengths of the desired product bands were further verified by imaging gels after Sybr Gold staining. Catalytic turnover of all hairpins was verified by the near-complete conversion of all primers to the last state, despite the hairpins being present at one-tenth the primer concentration.

To demonstrate how PER-synthesized strands can serve as elements for nanoconstruction, we sought to synthesize the staples for a DNA origami<sup>2</sup> structure in a one-pot reaction. A structure comprising a three-letter code scaffold held together by 40 staple strands was designed to fold into a compact rectangular shape that aggregates along its short end to produce chains of

origami structures. A total of 80 hairpins were designed to synthesize the 40 staple strands from 40 primers (Fig. 3D), each in two reaction steps (see Supplementary Section 4 for additional details). The 40 reaction cascades were all run in parallel by incubation with polymerase for 1 h at 37 °C. After heat inactivation, the scaffold strand was introduced directly into the PER mix and annealed for 1 h. The designed morphology of the resultant origami structures was then verified by visualization with atomic force microscopy (AFM; see Methods and Supplementary Sections 10 and 11).

We call the primer exchange reaction a ‘molecular primitive’ due to its generality, modularity and programmability (see Supplementary Section 5 for other examples of molecular primitives). Using the PER primitive, we can prescribe the number of steps as well as the sequence for each of these ordered steps in the reaction cascade. Additionally, the number of nucleotides added per step can be changed simply by including additional bases in the copy region of the PER hairpin’s stem. Note that the copy region can be much longer than the primer binding region, which is typically kept at 7–9 nt under our typical reaction conditions to simultaneously allow (1) efficient primer binding and priming for polymerization and (2) dissociation of the elongated transcript from the hairpin.

These features enable the PER cascade to be programmed to produce arbitrary user-prescribed sequences, as exemplified by the five-step synthesis in Fig. 3A–C, the simultaneous operation of 40 orthogonal two-step reaction cascades in Fig. 3D and the synthesis of a functional DNzyme in the next section.

**Nanodevice for conditional RNA degradation.** The DNA strand produced by PER cascades can serve as *in situ* synthesized, functional elements. In addition to serving as structural components to form nanostructures (for example, as staples for DNA origami as in Fig. 3D), the strands can also function as

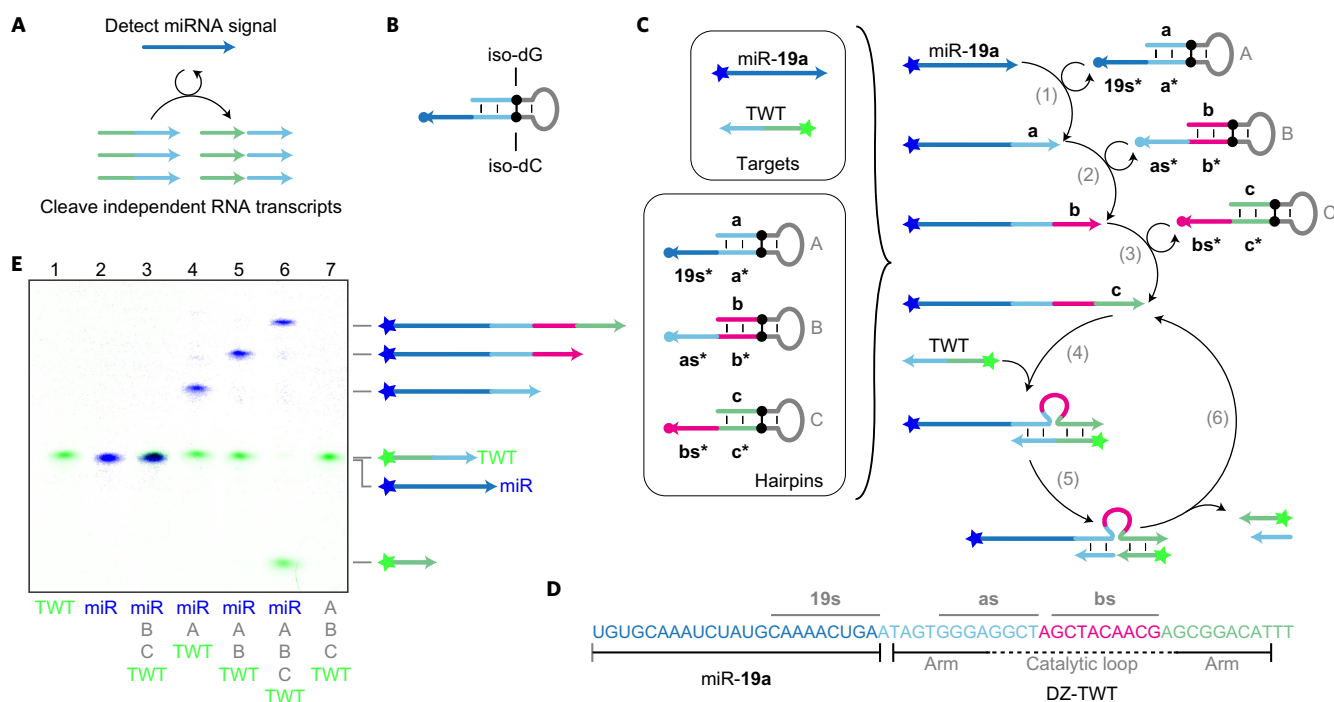


**Figure 4 | PER nanodevice for conditional RNA degradation.** **A**, Schematic for the nanodevice, which detects a miRNA target and cleaves an independent RNA transcript. **B**, Synthetic nucleotides, iso-dG and iso-dC, which are used as a stop sequence for four-letter code synthesis. **C**, System set-up and reaction diagram for the nanodevice. The oncogenic miR-19a sequence triggers cleavage of a fragment of the Twist mRNA sequence (TWT) through synthesis of a 10–23 DNAzyme sequence (DZ-TWT) by the A, B and C hairpins. **D**, Sequence breakdown of miRNA target (miR-19a) with DNAzyme (DZ-TWT) appended. Binding regions of the nascent primer strand are indicated by lines above the sequence, and the arms and catalytic domain of the DNAzyme are depicted below. **E**, PAGE denaturing gel validating the miRNA and Twist mRNA fragment states given different hairpins in the incubation solution. Reactions were incubated for 4 h at 37 °C with dNTPs at 10  $\mu$ M each. The miRNA target and hairpins B and C were at 10 nM and the TWT fragment and hairpin A were at 20 nM. See Methods for full experimental details.

chemically active species, as shown next. Additionally, the PER cascade can be programmed to initiate only when encountering specific molecular triggers. Using these features, we next demonstrate the construction of a PER nanodevice for conditional RNA degradation. More specifically, the nanodevice detects the oncogenic miR-19a signal and subsequently synthesizes a functional DNAzyme that is programmed to cut an independent RNA substrate (Fig. 4A). For target detection, we designed a hairpin to bind the shared 3' region of the oncogenic microRNAs (miRNAs) miR-19a and miR-19b<sup>49</sup>. In response to detection, a PER pathway synthesizes a DNAzyme (DZ-TWT) that has been shown to cleave the full-length mRNA of the Twist gene and promote apoptosis *in vivo*<sup>50</sup>.

For this application, a pair of synthetic nucleotides, iso-dG and iso-dC, were used as a stop sequence on all hairpins (Fig. 4B). This allowed us to use all four DNA bases in the synthesized sequences. As an example of an output construct for PER pathways, we chose to use the DZ-TWT DNAzyme, which has already been validated *in vivo*<sup>50</sup>. DZ-TWT is part of the class of 10–23 DNAzymes that use a 15 nt catalytic loop domain to cut a purine–pyrimidine bond in a target RNA sequence<sup>51</sup>. The catalytic loop is positioned at the cleavage site with the aid of two adjacent binding arms, whose sequences can be reprogrammed to bind to and cleave arbitrary RNA targets.

To implement the system logic, three PER hairpins were designed to synthesize the DZ-TWT sequence only upon detection of the target miRNA (Fig. 4C). When the target is present, the A hairpin directs the synthesis of domain **a** onto the target strand (step 1). The B and C hairpins can subsequently pattern the appendage of domains **b** and **c**, respectively (steps 2 and 3). The completed **a–b–c** sequence forms the DZ-TWT sequence, which can bind to a

24 nt fragment of the Twist mRNA sequence (TWT) to form a loop that catalyses the cleavage of the RNA at a particular base (steps 4 and 5). The DNAzyme can then be recycled after it dissociates from the cleaved fragments (step 6).

The sequences of the full DNAzyme appended to the target are shown in Fig. 4D. The three domains into which we split the DZ-TWT sequence are shown in different colours. The lengths of the primer binding sites on the hairpins (**19s\***, **as\*** and **bs\*** on hairpins A, B and C, respectively) were adjusted to bind 8–9 nt of the nascent strand to ensure the nascent strand would dissociate from hairpins after copying.

To evaluate the nanodevice function, we included different subsets of hairpins and the FAM-labelled TWT fragment with and without the Cy5-labelled miRNA target (Fig. 4E). Lanes 1 and 2 show the TWT fragment and miR-19a bands when incubated without any hairpins present. Lane 3 shows that there is no elongation of the miRNA in the presence of the last two hairpins, B and C, but not the first, A. Lane 4 shows the first step of extension when the miRNA is incubated with just the A hairpin and TWT fragment. Lane 5 shows incubation of the target with the first two hairpins, A and B, which results in two-step elongation. When the target is mixed with all three hairpins (lane 6), the full DZ-TWT sequence is appended to it and successfully cleaves the TWT fragment as expected. But when all the hairpins are mixed without target, no cleavage of the TWT fragment occurs (lane 7). Catalytic turnover of the DNAzyme construct is indicated by essentially complete cleavage of 20 nM TWT RNA with only 10 nM of miRNA target.

**Synthetic ‘telomerase’ as an *in situ* signal amplifier.** With the nanodevice, we were able to synthesize an arbitrary biologically relevant DNA sequence in response to an arbitrary input



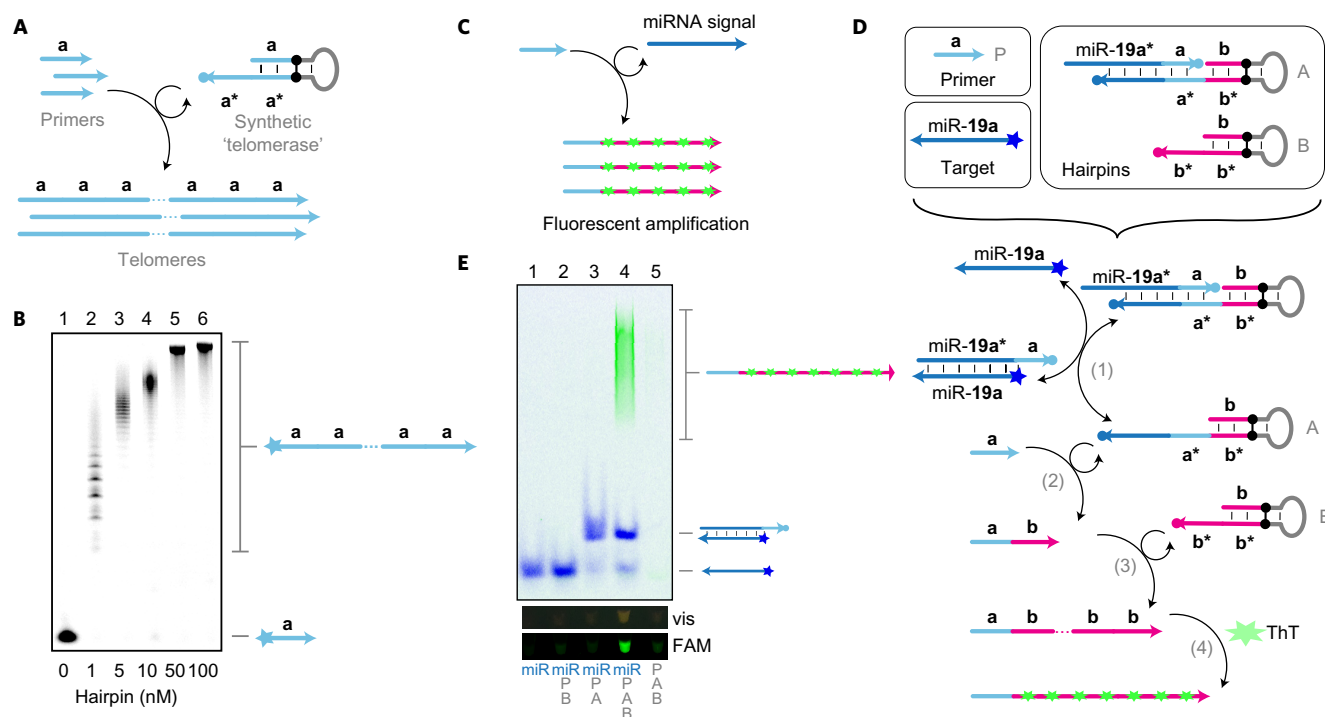


**Figure 5 | Signal amplifier with PER.** **A**, Schematic for implementing a synthetic ‘telomerase’ with a single PER hairpin. **B**, PAGE denaturing gel showing telomerization under different hairpin concentrations. 100 nM primers were incubated with the hairpins for 4 h at 37 °C with dATP, dTTP and dCTP at 100  $\mu$ M. **C**, Schematic for the signal amplifier, where a miRNA target activates the synthesis of fluorescent telomere strands. **D**, System components and reaction diagram for the signal amplifier. A gated hairpin (A) and telomerase hairpin (B) are designed to react to the detection of a miRNA signal and concatenate repeats of the human telomeric sequence *TTAGGG*, into which ThT intercalates. **E**, A native PAGE gel showing conditional telomerization in the presence of 10 nM miRNA signal for 4 h at 37 °C with dATP, dTTP and dGTP at 100  $\mu$ M. Primer P and hairpins A and B were held at 100 nM, 10 nM and 1  $\mu$ M, respectively. The protector for hairpin A was at 15 nM. Target detection can be visualized with a blue light transilluminator through the amber filter unit (vis) and on a Typhoon scanner (FAM). See Methods for additional details.

sequence. This programmability of PER pathways to transduce one sequence into another presents a modular framework for engineering environmentally responsive synthetic systems, which we explored further with several additional applications. We next implemented a single-hairpin system that synthesizes long strands of repeated sequence domains (Fig. 5A), which we call a synthetic ‘telomerase’, and then used this construct as a signal amplifier that grows fluorescent concatemers upon detecting a particular miRNA input (Fig. 5C).

The synthetic telomerase system comprises a single primer sequence (with domain **a**) and a hairpin that catalyses the appendage of a repeated domain **a** onto the growing strand (Fig. 5A). For this demonstration, we chose the 10 nt sequence *ATCTCTTATT* as the repeated domain, with the hairpin-binding region corresponding to the last 9 nt of the sequence. As before, the primer was labelled with a Cy5 fluorophore for gel visualization and the hairpin was fitted with an inverted dT on its 3' end to prevent its extension.

We validated the construct using an experimental set-up similar to that used in previous demonstrations, varying the hairpin concentration over two orders of magnitude to show how the reaction rate changes (Fig. 5B). Hairpins were incubated with the primer after 15 min of incubation with a specialized hairpin species designed to consume extraneous dGTP (see Supplementary Section 6 for details). Lane 1 shows the primer band with no hairpin added and lanes 2–6 show ‘telomeres’ grown with hairpin concentrations ranging from 1 to 100 nM. Increasing the hairpin concentrations resulted in longer telomeric sequences, which indicates the rate of telomerization can be tuned by adjusting the hairpin concentration. We also discovered that the magnesium concentration can be used to modulate the

telomerization rate, providing yet another method for adjusting reaction kinetics (Supplementary Section 7).

We subsequently devised a strategy for implementing a signal amplifier that could conditionally grow this type of telomeric output only in response to the presence of a particular miRNA signal (Fig. 5C). By designing the sequences to bind a particular fluorescent dye, we were able to make these synthesized telomeres fluorescent, allowing for direct visualization of the result under a blue light. The fluorescence was achieved through binding of the thioflavin T (ThT) dye, which has been shown to become more fluorescent once intercalated into the quadruplex motifs formed by repeats of the human telomeric sequence *TTAGGG*<sup>52</sup>. The target we chose was an oncogenic miRNA, miR-19a<sup>49</sup>.

Three components are required to implement the detector–telomerase system (Fig. 5D): a primer (P), a gated hairpin (A) and a telomerase hairpin (B). To transduce target detection into the synthesis of the human telomeric sequence, a toehold exchange reaction<sup>12,13</sup> was designed such that the primer binding site of a PER hairpin (A) is only exposed in the presence of the cognate miR-19a signal. The miRNA target can bind onto a short exposed domain on a protector strand bound to the A hairpin and branch migrate through the remaining complementary sequence. Once the complementary miR-19a\* domain has been fully displaced, the protector strand can spontaneously dissociate from the protected PER hairpin, exposing the primer binding site **a\*** on the A hairpin (step 1). Once exposed, this PER hairpin facilitates the appendage of the **b** domain onto the **a** domain of primer P (step 2). The **b** domain corresponds to the human telomeric sequence *TTAGGG*, which is subsequently telomerized by a constitutively active telomerase hairpin B (step 3). Finally, these telomeres form

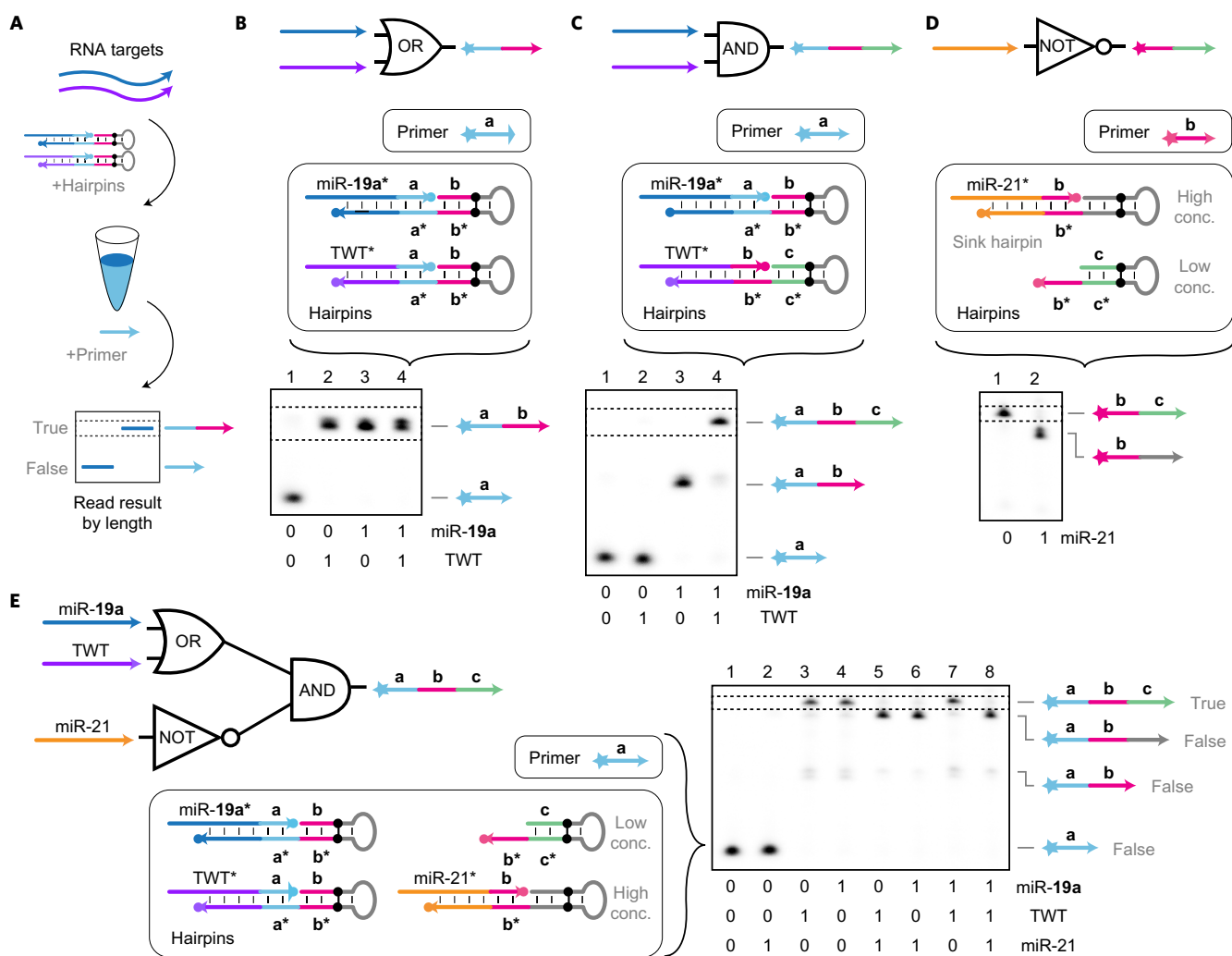


**Figure 6 | Logic computation with PER.** **A**, Operational schematic for evaluating logic expressions with RNA inputs. **B**, miR-19a OR TWT gate reaction components and a PAGE denaturing gel depicting transcript production in response to the different RNA inputs. True outputs are read by looking for transcripts of a particular length, indicated by dotted lines. **C–E**, Reaction set-up and PAGE denaturing gel results for miR-19a AND TWT (**C**), NOT miR-21 (**D**) and (miR-19a OR TWT) AND (NOT miR-21) (**E**). In all experiments, RNA targets and hairpin protectors were fixed at 250 nM final concentrations. Hairpins for **B** were at 100 nM. In **C**, 100 nM and 200 nM miR-19a and TWT hairpins were used, respectively. In **D**, the miR-21 sink hairpin was held at a concentration of 150 nM and the slow unprotected hairpin at 30 nM. In **E**, 100 nM miR-19a and TWT hairpins, 200 nM miR-21 sink hairpin and 40 nM slow unprotected hairpin were used. After 15 min of pre-incubation at 37 °C with the targets and protected hairpins, primers were introduced and incubated for 2 h, 2 h, 3 h and 5 h for **B–E**, respectively. All reactions used 10  $\mu$ M each of dATP, dTTP and dCTP. See Methods for additional details.

a quadruplex structure into which the ThT dye intercalates and becomes fluorescent (step 4).

The toehold exchange mechanism introduced here allows arbitrary input sequences to be connected to arbitrary primer exchange reactions using gated hairpins (Supplementary Section 8). This is a more modular and scalable approach than using the input sequence directly as the primer, as in Fig. 4, and expands the types of dynamic machinery that can be implemented with PER cascades, as each individual reaction can now be independently programmed to be conditioned upon different environmental signals. This is exemplified in the two molecular systems described in the following.

To evaluate the conditional telomerization reaction, we incubated reactions with different subsets of components and visualized the results on a native PAGE gel (see Methods for full details). Lane 1 in Fig. 5E shows a reaction with just the miRNA and none of the hairpins. With primer P and telomerase hairpin B, but no gated hairpin A, the miRNA target does not bind to any oligos and there is no telomerization (lane 2). With primer P and gated hairpin A, but no telomerase hairpin B, the miRNA binds to the

protector strand as indicated by the shift in its band (lane 3). Telomerization only occurs when all three of P, A and B are present with the miRNA target (lane 4). In the control reaction, which contains none of the miRNA target, elements P, A and B produce almost no background telomerization (lane 5).

As a simpler readout method, the fluorescence of the reactions can be visualized using a Safe Imager 2.0 Transilluminator through the amber filter unit (vis). This provides a safe, cost-effective and time-efficient manner of reading out the signal. The tubes may also be visualized on a fluorescence scanner under the FAM channel (see Methods for full details).

**Logic computation circuits.** Signal processing of target sequences through logic expression evaluation has emerged as a valuable framework for programming complex dynamic molecular behaviours<sup>12,16</sup>. In the following we show how PER can be used to implement AND, OR and NOT logic for arbitrary sequences simply by programming which primer sequences become appended based on the presence (or absence) of target strands.

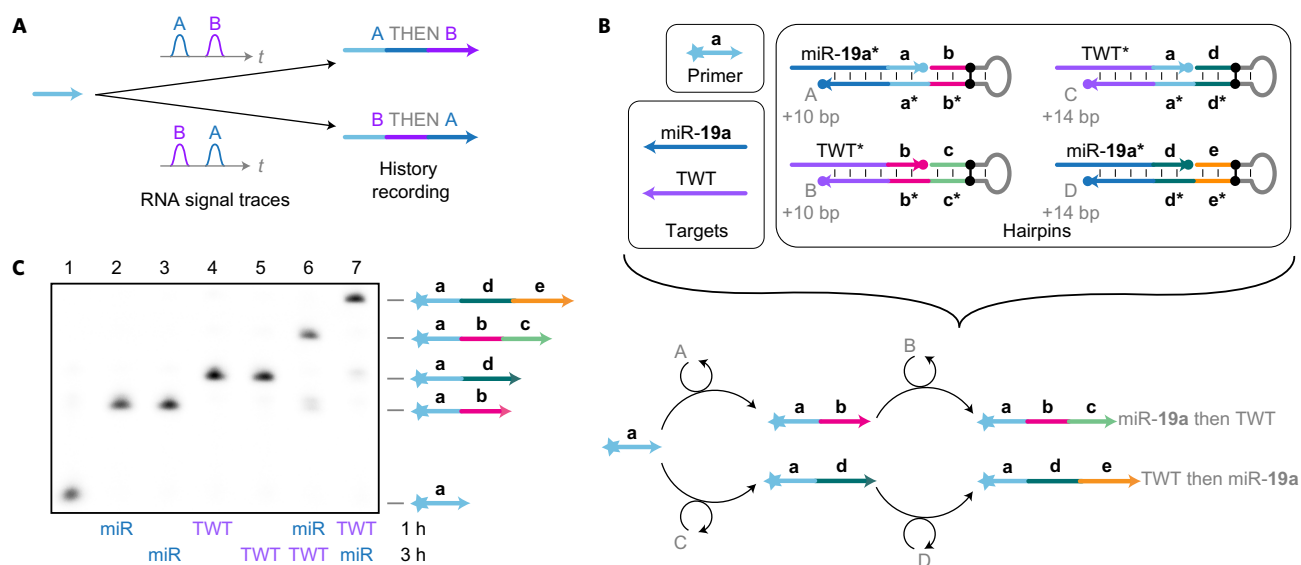


**Figure 7 | PER temporal molecular event recorder.** **A**, Schematic for an event recorder, which produces PER transcripts in response to time-varying RNA signals. **B**, System components and reaction diagram for the recorder. Four gated hairpins (A, B, C and D) are used to program the synthesis of different sequences in response to different orders of encountering two RNA targets: miR-19a and a fragment of the Twist mRNA (TWT). **C**, A PAGE denaturing gel showing transcripts of different lengths recorded for different 250 nM RNA signal spikes at 1 and 3 h into a 5 h reaction at 37 °C. Hairpins A and C were at 25 nM, protectors A and C at 50 nM, hairpins B and D at 75 nM, protectors B and D at 100 nM and primer at 100 nM. The reactions used 10  $\mu$ M each of dATP, dTTP and dCTP. All given concentrations are based on their final concentrations. See Methods for additional details.

The basic strategy is to equilibrate the RNA targets with the gated hairpins, introduce the primer and read out the result by length on a gel after incubation (Fig. 6A).

Figure 6B presents the design of an OR gate for two RNA inputs, which is implemented with two of the gated hairpins introduced in the previous section (Fig. 5D). Each target can activate one of the two hairpins and, when one or both of the two hairpins are activated, the **b** domain can be appended onto the primer's **a** domain. The results are validated with a denaturing gel, which shows no extended products when neither target is present (Fig. 6B, lane 1). However, if one or both targets are present, the primer is extended by one domain (lanes 2–4).

To evaluate whether two targets are both present (AND logic), their presence is checked in a stepwise manner (Fig. 6C). Primer domain **a** does not become extended if neither target is present (lane 1) or if just the TWT target is present (lane 2). If just the miR-19a target is present, the primer is extended by one domain to **a–b** (lane 3). However, if both targets are present, the primer is extended to the full **a–b–c** sequence, indicating successful evaluation of the AND expression (lane 4).

Implementing NOT logic requires a separation of timescales between target acceptance and rejection (Fig. 6D). This can be achieved by including a target-dependent sink reaction hairpin at a much higher concentration than the hairpin that evaluates to True (**b–c**). Thus, if the target, miR-21 in this case, is present, then the **b** primers are funnelled into an inactive (grey) state. However, if no target is present, at a slow rate all of the **b** primers will be converted to **b–c**. The gate is validated by comparing incubation results without (lane 1) and with (lane 2) the target, respectively.

Finally, we demonstrated that several of these types of gate can be hooked together to compute the expression (miR-19a OR TWT) AND (NOT miR-21) (Fig. 6E). This computation is achieved by cascading the result of the (miR-19a OR TWT) gate from Fig. 6B into the NOT miR-21 gate from Fig. 6D. The results were validated as before through gel electrophoresis. Primers remain predominantly in their unextended state when either no inputs or just the miR-21 target are present (lanes 1 and 2). When either just the TWT or just the miR-19a is present, the expression

evaluates to True, as indicated by the fully extended **a–b–c** product (lanes 3 and 4). However, when one of these is present in addition to miR-21, the primer is funnelled into an inactive state (lanes 5 and 6). Having both miR-19a and TWT but no miR-21 again results in a True result (lane 7), but when all three targets are present the expression again evaluates to False (lane 8).

These circuit components demonstrate the modularity of the PER method. The results of one logical evaluation can be cascaded easily into another by matching synthesized and binding primer domains, and this type of reconfiguration could in principle be extended to any primer domain given any single-stranded RNA or DNA inputs.

**Temporal molecular event recorder.** We next created a temporal molecular event recording system that encodes the sequential order in which two RNA targets are encountered into dynamically synthesized transcripts (Fig. 7A).

Each of the four hairpins used in this application utilizes the same method of toehold exchange for target detection as the signal amplifier and logic circuits. Depending on the order in which the two RNA signals are introduced, a primer will undergo one of two elongation pathways (Fig. 7B). If miR-19a is introduced first, then the initial primer is extended with **b** via hairpin A. If the TWT target is then introduced, hairpin B can append **c** to the primer. If, on the other hand, TWT is introduced first, then **d** is added to the **a** primer sequence with the exposed C hairpin, and hairpin D can then append **e** if the miR-19a signal is encountered later.

Because the hairpins are designed to copy different numbers of nucleotides per addition, differentiation of the sequence length is achieved based on the order in which the signals are introduced in solution. These results can be read out on a PAGE denaturing gel (Fig. 7C). By introducing signals at either 1 or 3 h into a 5 h incubation with the primer and hairpins A–D, the recording behaviour was evaluated. Lane 1 shows the system with no targets introduced and shows no extension due to the continuous protection of all four hairpins. Lanes 2 and 3 show a single extension of a 10 nt step patterned by hairpin A when miR-19a (miR) was introduced

at 1 and 3 h, respectively. Introducing TWT at 1 or 3 h results in a single extension of 14 nt by the exposed C hairpin (lanes 4 and 5). Introducing the miRNA first and then TWT results in two 10 nt extensions to form the **a–b–c** sequence. Finally, introducing first the TWT target and then the miRNA results in two 14 nt extension steps to form **a–d–e**, thus validating our ability to read out the temporal relationship of the two RNA signals in the length of synthesized DNA.

## Discussion

PER dynamically synthesizes arbitrary prescribed DNA sequences in an autonomous and stepwise fashion. PER cascades are programmed using catalytic PER hairpins, driven by polymerase, fuelled by dNTPs and happen in a homogeneous solution under isothermal conditions. PER allows arbitrary sequences to be concatenated into a desired transcript, reactions can be simply cascaded together to form prescribed growth pathways, and the synthesis can be made responsive to current environmental conditions. Together, these features make PER a versatile programmable platform for implementing diverse environmentally responsive molecular behaviours (for example, the conditional RNA degrader, the *in situ* signal amplifier, the logic RNA expression profiler and the temporal recorder constructed in this Article).

PER provides a new platform for engineering synthetic DNA circuits and devices, expanding and complementing existing methods such as those based on toehold-mediated branch migration<sup>53,54</sup>, which has been the dominant mechanism for implementing dynamic DNA devices and circuits. Toehold-based circuits and devices rely on dynamic conditional assembly and disassembly of presynthesized materials (that is, DNA strands), whereas PER circuits primarily rely on conditional dynamic synthesis of new materials (that is, DNA strands). Toehold circuits are typically engineered via controlled spatial concealing and revealing of cascading nucleation sites (that is, toeholds) and are fuelled by association (that is, DNA hybridization-driven) or dissociation (that is, entropy-driven) of presynthesized units, while PER circuits are engineered via controlled chemical synthesis of cascading nucleation sites (that is, primers) and are fuelled by polymerization of dNTP monomers.

Although both toehold and PER mechanisms can be used to engineer diverse dynamic behaviours, PER appears to be more compact in terms of its usage for construction materials (by avoiding using auxiliary strand fragments to effectively sequester toeholds from interacting with other metastably existing complements in the system) and fuels (by using dNTP monomers rather than DNA strands). The compactness and simplicity of PER, for example, enables the facile design and construction of 40 orthogonal PER circuits for the *in situ* synthesis of DNA origami staples (Fig. 3D) and a single small hairpin-based-signal amplification circuit (synthetic ‘telomerase’ in Fig. 5).

To construct dynamic circuits, both toehold and PER mechanisms need to engineer kinetic barriers, which are essential for manipulating the reaction system’s free energy landscape to achieve desired component metastability. Toehold circuits implement these barriers by manipulating weak bonds and hence tend to suffer leakage, which is the unintended off-pathway reaction in the absence of the trigger, typically caused by suboptimal spatial shielding of the pre-synthesized toeholds, for example, due to ‘breathing’ of the DNA duplex of toeholds’ incumbent and vicinity regions. PER circuits, by implementing such kinetic barriers via the manipulation of covalent bonds, promise, in principle, to deliver steeper kinetic barriers and thus to mitigate the leakage problem. Although a comprehensive and rigorous comparison of leakage in toehold versus PER systems is still under way, the initial indication of PER’s resistance to leakage comes from a lack of detectable extension of a non-cognate primer in the presence of the highest hairpin

concentration used for the synthetic ‘telomerase’ system (for example, Supplementary Fig. 16).

PER differs from previous demonstrations of various polymerase-based synthetic DNA circuits and molecular computing schemes in that it provides a general method for autonomous programmable synthesis of single-stranded DNA in an environmentally responsive fashion and thus enables the construction of diverse synthetic dynamic devices beyond molecular information processing. Notable previous examples include the Polymerase/Exonuclease/Nickase Dynamic Network Assembly toolbox (or PEN DNA toolbox for short)<sup>41,42</sup> and Whiplash PCR<sup>55–59</sup>. The PEN DNA toolbox uses sophisticated coordination of polymerase, exonuclease and nicking enzymes to achieve the controlled generation of primer cascades to implement various computing functions (for example, oscillations<sup>41,60</sup> and spatial patterns such as spirals and travelling waves<sup>61,62</sup>). Unlike PER, which uses the catalytic PER hairpin to append independent primers to existing primers, the PEN DNA toolbox typically generates a new cascading primer without concatenating it to the previous one and hence is not suitable for the continuous growth of a nascent strand with arbitrary user-prescribed sequence. Additionally, the reliance on various nucleases puts constraints on the sequences (for example, enzyme recognition sites) that may be produced. Therefore, PEN reactions have similar cascading capabilities, but the concatenation of sequences together with PER cascades enables the synthesis of new functional materials. These outputs can serve as structural elements (for example, origami staples and fluorescent scaffolds), functional elements (for example, DNAszymes) and records (for example, logic transcripts and history records). In contrast, the diffusible outputs of PEN cascades are still limited to being exact copies of existing sequences in solution. Whiplash PCR<sup>55–59</sup> uses polymerase to append a new primer ‘state’ domain to an existing one based on a set of state transition rules for performing a particular computing function and as a consequence grows a DNA strand that encodes the state transition history. Although suitable for implementing state transition-based computing, Whiplash PCR typically involves staged external manipulation or thermal cycling to achieve successive transition and hence strand extension, with limited experimental demonstrations. Theoretical schemes (for example, in refs 57,59) for isothermal, autonomous operation have been proposed, but not experimentally validated. Additionally, the strand extension is a by-product of implementing the desired molecular computing, rather than the primary purpose, so its general suitability as an autonomous programmable strand synthesis method remains to be explored.

In addition to RNA inputs and the fluorescence and DNAszyme outputs demonstrated here, PER reactions could be interfaced with other diverse environmental triggers and actuation functions, for example to detect protein input via aptamers<sup>63</sup> or programming protein synthesis output via toehold switches<sup>64</sup>. PER could also be directly interfaced with the rich set of DNA strand displacement circuits<sup>54</sup>. The programmable sensing, processing, recording and actuation capabilities of PER circuits could thus unleash a new generation of molecular programming devices and applications. One particularly interesting example would be molecular recording: as long polymers can be grown following different pathways depending on the current state of the environment, PER devices could be programmed to record environmental signals over extended periods of time and the resultant transcripts could be sequenced to recover the molecular event reports.

## Methods

**DNA synthesis and purification.** All oligos were ordered from IDT, either unpurified or HPLC-purified. Purified RNA molecules were ordered purified with RNase-free HPLC. Some unpurified oligos were purified in-house by running 100  $\mu$ l of 100  $\mu$ M unpurified oligo through a Qiagen MinElute PCR purification column and washed according to the kit instructions. Column-bound oligos were eluted to 15  $\mu$ l and concentrations were measured using a Nanodrop and their extinction



coefficients. Oligos were ordered pre-suspended in 1× TE buffer (10 mM Tris, 0.1 mM or 1.0 mM EDTA) buffer at 100 μM, and these concentrations were assumed for all dilutions, with the exception of MinElute purified oligos. All oligos were diluted in 1× TE to working concentrations of 10 μM, with stock and working solutions of DNA stored at –20 °C and RNA stored at –80 °C. Oligo sequences for all experiments are listed in Supplementary Section 9.

**PER incubation.** All PER experiments were incubated at 37 °C for the indicated amount of time, usually with 1× ThermoPol buffer with supplemented magnesium (20 mM Tris-HCl, 10 mM (NH<sub>4</sub>)<sub>2</sub>SO<sub>4</sub>, 10 mM KCl, 12 mM MgSO<sub>4</sub> and 0.1% Triton X-100), 0.8 units per μl of Bst Large Fragment polymerase and 10–100 μM of the appropriate dNTPs. Typically, 20 μl reactions were quenched by heat inactivation of the enzyme at 80 °C for 20 min and loaded with 10 μl formamide. For RNA-sensitive samples, reactions were instead quenched with EDTA. For the signal amplifier, reactions were not quenched but were loaded directly after incubation. Some experiments were pre-incubated for 15 min to allow the solution to equilibrate. See Supplementary Section 10 for the reaction details for each experiment.

**Gel electrophoresis.** Most experiments used 15% TBE-urea PAGE denaturing gels, which were run at 200 V for 35 min at 65 °C and scanned with the Cy5 and FAM channels. Gels were also stained with Sybr Gold for several minutes and subsequently imaged with the Sybr Gold channel (see Supplementary Figs 12–29 in Supplementary Section 11 for the gel scans of all experiments). Some experiments used different gel conditions (see Supplementary Section 10 for details).

**AFM.** AFM imaging was performed on a Nanoscope V machine.

**Sequence design.** Most sequences were designed using in-house Python optimization code paired with command line NUPACK executables<sup>65</sup>. The NUPACK web application<sup>66,67</sup> was also used to analyse constructs.

**Data availability.** The principal data supporting the findings of this work are available within the figures and the Supplementary Information. All other data are available from the corresponding author upon request.

Received 4 February 2017; accepted 6 September 2017;  
published online 6 November 2017

## References

- Winfree, E., Liu, F., Wenzler, L. A. & Seeman, N. C. Design and self-assembly of two-dimensional DNA crystals. *Nature* **394**, 539–544 (1998).
- Rothemund, P. W. K. Folding DNA to create nanoscale shapes and patterns. *Nature* **440**, 297–302 (2006).
- Douglas, S. M. *et al.* Self-assembly of DNA into nanoscale three-dimensional shapes. *Nature* **459**, 414–418 (2009).
- Zheng, J. *et al.* From molecular to macroscopic via the rational design of a self-assembled 3D DNA crystal. *Nature* **461**, 74–77 (2009).
- Wei, B., Dai, M. & Yin, P. Complex shapes self-assembled from single-stranded DNA tiles. *Nature* **485**, 623–626 (2012).
- Ke, Y., Ong, L. L., Shih, W. M. & Yin, P. Three-dimensional structures self-assembled from DNA bricks. *Science* **338**, 1177–1183 (2012).
- Han, D. *et al.* DNA gridiron nanostructures based on four-arm junctions. *Science* **339**, 1412–1415 (2013).
- Gerling, T., Wagenbauer, K. F., Neuner, A. M. & Dietz, H. Dynamic DNA devices and assemblies formed by shape-complementary, non-base pairing 3D components. *Science* **347**, 1446–1452 (2015).
- Benson, E. *et al.* DNA rendering of polyhedral meshes at the nanoscale. *Nature* **523**, 441–444 (2015).
- Dunn, K. E. *et al.* Guiding the folding pathway of DNA origami. *Nature* **525**, 82–86 (2015).
- Veneziano, R. *et al.* Designer nanoscale DNA assemblies programmed from the top down. *Science* **352**, 1534 (2016).
- Seelig, G., Soloveichik, D., Zhang, D. Y. & Winfree, E. Enzyme-free nucleic acid logic circuits. *Science* **314**, 1585–1588 (2006).
- Zhang, D. Y., Turberfield, A. J., Yurke, B. & Winfree, E. Engineering entropy-driven reactions and networks catalyzed by DNA. *Science* **318**, 1121–1125 (2007).
- Yin, P., Choi, H. M. T., Calvert, C. R. & Pierce, N. A. Programming biomolecular self-assembly pathways. *Nature* **451**, 318–322 (2008).
- Omabegho, T., Sha, R. & Seeman, N. C. A bipedal DNA Brownian motor with coordinated legs. *Science* **324**, 67–71 (2009).
- Qian, L. & Winfree, E. Scaling up digital circuit computation with DNA strand displacement cascades. *Science* **332**, 1196–1201 (2011).
- Chirieleison, S. M., Allen, P. B., Simpson, Z. B., Ellington, A. D. & Chen, X. Pattern transformation with DNA circuits. *Nat. Chem.* **5**, 1000–1005 (2013).
- Weitz, M. *et al.* Diversity in the dynamical behaviour of a compartmentalized programmable biochemical oscillator. *Nat. Chem.* **6**, 295–302 (2014).
- Karzbrun, E., Tayar, A. M., Noireaux, V. & Bar-Ziv, R. H. Programmable on-chip DNA compartments as artificial cells. *Science* **345**, 829–832 (2014).
- Mohammed, A. M., Šulc, P., Zenk, J. & Schulman, R. Self-assembling DNA nanotubes to connect molecular landmarks. *Nat. Nanotech.* **12**, 312–316 (2016).
- Choi, H. M. T. *et al.* Programmable *in situ* amplification for multiplexed imaging of mRNA expression. *Nat. Biotechnol.* **28**, 1208–1212 (2010).
- Zhang, D. Y., Chen, S. X. & Yin, P. Optimizing the specificity of nucleic acid hybridization. *Nat. Chem.* **4**, 208–214 (2012).
- Douglas, S. M., Bachelet, I. & Church, G. M. A logic-gated nanorobot for targeted transport of molecular payloads. *Science* **335**, 831–834 (2012).
- Kuzyk, A. *et al.* DNA-based self-assembly of chiral plasmonic nanostructures with tailored optical response. *Nature* **483**, 311–314 (2012).
- Derr, N. D. *et al.* Tug-of-war in motor protein ensembles revealed with a programmable DNA origami scaffold. *Science* **338**, 662–665 (2012).
- Jungmann, R. *et al.* Multiplexed 3D cellular super-resolution imaging with DNA-PAINT and exchange-PAINT. *Nat. Methods* **11**, 313–318 (2014).
- Sun, W. *et al.* Casting inorganic structures with DNA molds. *Science* **346**, 1258361 (2014).
- Wang, J. S. & Zhang, D. Y. Simulation-guided DNA probe design for consistently ultraspecific hybridization. *Nat. Chem.* **7**, 545–553 (2015).
- Gopinath, A., Miyazono, E., Faraon, A. & Rothemund, P. W. K. Engineering and mapping nanocavity emission via precision placement of DNA origami. *Nature* **535**, 401–405 (2016).
- Bhatia, D. *et al.* Quantum dot-loaded monofunctionalized DNA icosahedra for single-particle tracking of endocytic pathways. *Nat. Nanotech.* **11**, 1112–1119 (2016).
- Kilchherr, F. *et al.* Single-molecule dissection of stacking forces in DNA. *Science* **353**, aaf5508 (2016).
- Nickels, P. C. *et al.* Molecular force spectroscopy with a DNA origami-based nanoscopic force clamp. *Science* **354**, 305–307 (2016).
- Walker, G. T. *et al.* Strand displacement amplification—an isothermal, *in vitro* DNA amplification technique. *Nucleic Acids Res.* **20**, 1691–1696 (1992).
- Lizardi, P. M. *et al.* Mutation detection and single-molecule counting using isothermal rolling-circle amplification. *Nat. Genet.* **19**, 225–232 (1998).
- Notomi, T. *et al.* Loop-mediated isothermal amplification of DNA. *Nucleic Acids Res.* **28**, e63 (2000).
- Wang, H. H. *et al.* Programming cells by multiplex genome engineering and accelerated evolution. *Nature* **460**, 894–898 (2009).
- Du, Y. & Dong, S. Nucleic acid biosensors: recent advances and perspectives. *Anal. Chem.* **89**, 189–215 (2017).
- Church, G. M., Gao, Y. & Kosuri, S. Next-generation digital information storage in DNA. *Science* **337**, 1628 (2012).
- Kosuri, S. & Church, G. M. Large-scale *de novo* DNA synthesis: technologies and applications. *Nat. Methods* **11**, 499–507 (2014).
- Saiki, R. K. *et al.* Primer-directed enzymatic amplification of DNA with a thermostable DNA polymerase. *Science* **239**, 487–491 (1988).
- Montagne, K., Plasson, R., Sakai, Y., Fujii, T. & Rondelez, Y. Programming an *in vitro* DNA oscillator using a molecular networking strategy. *Mol. Syst. Biol.* **7**, 466 (2011).
- Baccouche, A., Montagne, K., Padirac, A., Fujii, T. & Rondelez, Y. Dynamic DNA-toolbox reaction circuits: a walkthrough. *Methods* **67**, 234–249 (2014).
- Lee, C. S., Davis, R. W. & Davidson, N. A physical study by electron microscopy of the terminally repetitive, circularly permuted DNA from the coliphage particles of *Escherichia coli* 15. *J. Mol. Biol.* **48**, 1–22 (1970).
- Schau, T. E., Woo, S., Xuan, F., Chen, X. & Yin, P. A DNA nanoscope via auto-cycling proximity recording. *Nat. Commun.* **8**, 696 (2017).
- Newton, C. R. *et al.* The production of PCR products with 5′ single-stranded tails using primers that incorporate novel phosphoramidite intermediates. *Nucleic Acids Res.* **21**, 1155–1162 (1993).
- Sakamoto, K. *et al.* State transitions by molecules. *Biosystems* **52**, 81–91 (1999).
- Whitcombe, D., Theaker, J., Guy, S. P., Brown, T. & Little, S. Detection of PCR products using self-probing amplicons and fluorescence. *Nat. Biotechnol.* **17**, 804–807 (1999).
- Aubert, N., Rondelez, Y., Fujii, T. & Hagiya, M. Enforcing logical delays in DNA computing systems. *Nat. Comput.* **13**, 559–572 (2014).
- Grillari, J., Hackl, M. & Grillari-Voglauer, R. miR-17-92 cluster: ups and downs in cancer and aging. *Biogerontology* **11**, 501–506 (2010).
- Hjiantoniou, E., Iseki, S., Uney, J. B. & Phylactou, L. A. DNzyme-mediated cleavage of twist transcripts and increase in cellular apoptosis. *Biochem. Biophys. Res. Commun.* **300**, 178–181 (2003).
- Santoro, S. W. & Joyce, G. F. A general purpose RNA-cleaving DNA enzyme. *Proc. Natl Acad. Sci. USA* **94**, 4262–4266 (1997).
- Mohanty, J. *et al.* Thioflavin T as an efficient inducer and selective fluorescent sensor for the human telomeric G-quadruplex DNA. *J. Am. Chem. Soc.* **135**, 367–376 (2012).
- Yurke, B., Turberfield, A. J., Mills, A. P., Simmel, F. C. & Neumann, J. L. A DNA-fuelled molecular machine made of DNA. *Nature* **406**, 605–608 (2000).
- Zhang, D. Y. & Seelig, G. Dynamic DNA nanotechnology using strand-displacement reactions. *Nat. Chem.* **3**, 103–113 (2011).

55. Hagiya, M., Arita, M., Kiga, D., Sakamoto, K. & Yokoyama, S. in *DNA Based Computers III* Vol. 48 (eds Rubin, H. & Wood, D. H.) 57–72 (DIMACS Series in Discrete Mathematics and Theoretical Computer Science, American Mathematical Society, 1999).
56. Winfree, E. *Whiplash PCR for O(1) Computing* Technical Report 1998.23 (Caltech, 1998).
57. Rose, J. A., Deaton, R. J., Hagiya, M. & Suyama, A. in *DNA Computing* (Jonoska, N. & Seeman, N. C.) 104–116 (Springer, 2002).
58. Komiya, K., Yamamura, M. & Rose, J. A. in *International Workshop on DNA-Based Computers* 1–10 (Springer, 2008).
59. Reif, J. H. & Majumder, U. Isothermal reactivating whiplash PCR for locally programmable molecular computation. *Nat. Comput.* **9**, 183–206 (2010).
60. Fujii, T. & Rondelez, Y. Predator–prey molecular ecosystems. *ACS Nano* **7**, 27–34 (2012).
61. Padirac, A., Fujii, T., Estévez-Torres, A. & Rondelez, Y. Spatial waves in synthetic biochemical networks. *J. Am. Chem. Soc.* **135**, 14586–14592 (2013).
62. Zadorin, A. S., Rondelez, Y., Galas, J.-C. & Estevez-Torres, A. Synthesis of programmable reaction-diffusion fronts using DNA catalyzers. *Phys. Rev. Lett.* **114**, 068301 (2015).
63. Dirks, R. M. & Pierce, N. A. Triggered amplification by hybridization chain reaction. *Proc. Natl Acad. Sci. USA* **101**, 15275–15278 (2004).
64. Green, A. A., Silver, P. A., Collins, J. J. & Yin, P. Toehold switches: *de-novo*-designed regulators of gene expression. *Cell* **159**, 925–939 (2014).
65. Dirks, R. M., Bois, J. S., Schaeffer, J. M., Winfree, E. & Pierce, N. A. Thermodynamic analysis of interacting nucleic acid strands. *SIAM Rev.* **49**, 65–88 (2007).
66. Zadeh, J. N. *et al.* NUPACK: analysis and design of nucleic acid systems. *J. Comput. Chem.* **32**, 170–173 (2011).
67. Wolfe, B. R. & Pierce, N. A. Sequence design for a test tube of interacting nucleic acid strands. *ACS Synth. Biol.* **4**, 1086–1100 (2014).

## Acknowledgements

The authors thank W. Shih, J. Kim, X. Chen, N. Hanikel, E. Winfree, B. Beliveau and N. Liu for their discussions and comments. This work was supported by the Office on Naval Research (grants N000141310593, N000141410610, N000141612182 and N000141612410), the National Science Foundation (grants CCF1317291, CMMI1334109 and 1540214), the National Institutes of Health (grant 1R01EB01865901) and the Wyss Institute's Molecular Robotics Initiative. J. Kishi was supported by an NSF graduate research fellowship and T. Schaus was supported by the Jane Coffin Childs Postdoctoral Fellowship.

## Author contributions

J.Y.K. conceived and designed the study, designed and performed the experiments, analysed the data and wrote the manuscript. T.E.S. designed and performed the experiments and analysed the data. N.G. designed and performed the experiments and analysed the data. F.X. designed and performed the experiments and analysed the data. P.Y. conceived and supervised the study, interpreted the data and wrote the manuscript. All authors reviewed, edited and approved the manuscript.

## Additional information

Supplementary information is available in the [online version of the paper](#). Reprints and permissions information is available online at [www.nature.com/reprints](http://www.nature.com/reprints). Publisher's note: Springer Nature remains neutral with regard to jurisdictional claims in published maps and institutional affiliations. Correspondence and requests for materials should be addressed to P.Y.

## Competing financial interests

A provisional US patent has been filed based on this work. P.Y. is co-founder of Ultivue Inc. and NuProbe Global.